The American Journal of Pathology, Vol. 175, No. 5, November 2009

DOI: 10.2353/ajpath.2009.090257

Neurobiology

Unilateral Blood Flow Decrease Induces Bilateral and Symmetric Responses in the Immature Brain

Sonia Villapol,* Philippe Bonnin,† Sébastien Fau,*‡ Olivier Baud,§ Sylvain Renolleau,*‡ and Christiane Charriaut-Marlangue*

From the UMR-Centre de la Recherche Scientifique 7102, Equipe Hypoxie et Ischemie du Cerveau en Development, Paris; Assistance Publique-Hopitaux de Paris,† Hôpital Lariboisière, Physiologie-Explorations Fonctionnelles, Université-Denis Diderot-Paris7, INSERM U965, Paris; AP-HP,‡ Service de Réanimation, Hôpital Armand Trousseau, UPMC-Paris6, Paris; and INSERM U676,§ Equipe AVENIR R05230HS, Hôpital R. Debré, Paris, France*

The effects of hemodynamic changes in the developing brain have yet to be fully understood. The aim of this study was to explore the relationship between perturbations of the cerebral blood flow in the developing brain via unilateral hypoperfusion in P7 rats. As expected, nuclear caspase-3 (casp3) cleavage and DNA fragmentation were detected at 48 hours after stroke in the injured cortex. Surprisingly, casp3 was also cleaved in the contralateral cortex, although without cell death markers. Delayed (48 hours) casp3 cleavage without DNA fragmentation was also identified after unilateral common carotid artery occlusion, both in the hypoperfused cortex and the unaffected cortex, producing mirror images. Upstream calpain activation, caspase-2 cleavage, and mitochondrial cytochrome *c* release initiated casp3 cleavage, but did not produce preconditioning. The neuronal marker NeuN co-localized with cleaved casp3 in cortical layers II–III and VI and with gaba-amino butyric acid in layer III. Indeed, collateral supply was provided from the opposite side during carotid artery occlusion but not after reperfusion, and the number of cleaved casp3-positive cells significantly negatively correlated with the common carotid artery immediate reperfusion percentage. In summary, unilateral hypoperfusion, while insufficient to induce cell death, may active bilateral and symmetric casp3 in the P7 rat brain. Additionally, the opposite healthy hemisphere is altered due to the injury and thus should not be used as an internal control. ***(Am J Pathol 2009, 175:2111–2120; DOI: 10.2353/ajpath.2009.090257)***

Perinatal hypoxia-ischemia followed by reperfusion is an important cause of neonatal brain injury. In approximately 8 out of 100,000 children affected, it results in cerebral palsy, learning disabilities, visual field deficits, and epilepsy.[1] However, recent data suggest a higher incidence of focal ischemia in neonates compared with the incidence of global cerebral ischemia arising from systemic asphyxia,[2,3] whereas mechanisms of arterial ischemic injury without the confounding effect of hypoxia are not fully understood.

To investigate cell death pathways and neuroprotection, the most commonly used model of hypoxia-ischemia (HI)[4] and others stroke models[5,6] have been designed in the developing brain (age range from P3 up to P12) in both rats and mice. In all of these models, injury is only seen in the ipsilateral hemisphere and in a great number of studies the contralateral hemisphere was used as an internal control. However, two recent studies have pointed out that multiple molecular/cellular mediators were also activated in the contralateral hemisphere. In the first work, HI in P12 rats produced increased cytokine expression, hypoxic-inducing factor (HIF-1) α, and phospho (p)-Akt to the same extent in both hemispheres, although injury was unilateral. Conversely, hypoxia alone was sufficient to regulate these mediators, but not sufficient to induce long-term damage.[7] In the second study, we demonstrated that after stroke (electrocoagulation of the left middle cerebral artery (MCA) in association with transient homolateral common carotid artery occlusion) in P7 rats,[6] cell injury was visible in the ipsilateral (IL) parietal cortex, but cell death also affected the contralateral white matter during the first 24 hours of recovery followed

Supported by Prof. J. Mariani and the Centre de la Recherche Scientifique (UMR 7102) and the Agence Nationale pour la Recherche (ANR-06-BYOS-0002-03). S.V. is financially supported by a "Mairie de Paris" postdoctoral grant. We thank the foundation "Grace de Monaco" for funds donated toward the purchase of a Zeiss surgical microscope.

Accepted for publication July 23, 2009.

Supplemental material for this article can be found on *http://ajp.amjpathol.org*.

Address reprint requests to Christiane Charriaut-Marlangue, Ph.D., INSERM U676, Equipe AVENIR R05230HS, Hopital Robert Debré. Bâtiment Ecran - 3ème étage, 48 Bd Sérurier, 75019 Paris, France. E-mail: christiane.marlangue@gmail.com.

Table 1. Description of the Models Used

Animal model	Artery occlusion	Model description	No. of animals*
M1	pMCAo + uni-tCCAo	Left middle cerebral artery occlusion (MCAo) and unilateral transient left Common Carotid Artery occlusion (tCCAo)	$n = 27$
M2	Uni-t/pCCAo	Unilateral transient or permanent† left or right Common Carotid Artery occlusion (t/pCCAo)	$n = 21$
M3	Bi-tCCAo	Bilateral transient common carotid artery occlusion	$n = 6$
M4	Bi-pCCAo	Bilateral permanent common carotid artery occlusion	$n = 8$
M5	Uni-tCCAo 24 hours after pMCAo + uni-tCCAo	Unilateral transient common carotid artery occlusion (uni-tCCAo) and 24 hours after Left middle cerebral artery occlusion (MCAo) with uni-tCCAo	$n = 6$

*Tissues from animals were used either for immunohistochemistry or Western blotting analyses.
†Animals with permanent CCAo provided either from animals, who after CCAo release, did not show recanalization (determined after CBF measurements) or from animals with unilateral ligated CCA.

by delayed repair mechanisms in both the IL and contralateral (CL) hemispheres.[8] Because the molecular mechanisms of cell death/survival in remote regions and particularly in the CL hemisphere are still poorly understood, the aim of this study was to explore the relationship between the molecular pathways and perturbations of the cerebral blood flow (CBF) in the developing brain.

Arterial occlusion causes hemodynamic perturbations and a redistribution of blood flow. The circulatory system can compensate for this by various processes, for example, using collateral circulation and/or autoregulatory mechanisms.[9] However, the reserve capacity of the circulatory system is limited, and when these processes offer insufficient compensation, inevitably tissue will enter a state of hypoperfusion. This study highlights that unilateral hypoperfusion, not sufficient to induce cell death, may active cellular mechanisms bilaterally and symmetrically producing images in mirror in P7 rat brain.

Materials and Methods

Perinatal Ischemia

All animal experimentation was conducted in accordance with the French and European Community guidelines for the care and use of experimental animals. Ischemia was performed on 7-day-old rat pups (17 to 21 g, both sexes), as described previously.[6] Rat pups were anesthetized with an i.p. injection of chloral hydrate (350 mg/kg). The anesthetized rat was positioned on its back, and a median incision was made in the neck to expose the left common carotid artery (CCA). The rat was then placed on its right side and an oblique skin incision was made between the ear and the eye. After excision of the temporal muscle, the cranial bone was removed from the frontal suture to a level below the zygomatic arch. Then the left MCA, exposed just after its appearance over the rhinal fissure, was electrocoagulated (MCAo) at the inferior level of the cerebral vein. After this procedure, a vascular clip (18055-04; Fine Science Tools, Heidelberg, Germany) was placed to occlude the left common carotid artery (tCCAo). Rats were then placed in an incubator to avoid hypothermia. After 50 minutes, the clip was removed. Carotid blood flow restoration was verified with the aid of a microscope. This stroke model is referred to as model M1 (see Table 1). Both neck and cranial skin incisions were then closed. During the surgical procedure, external body temperature was maintained at 37–37.5°C. After recovery, pups were transferred to their mothers. In other sets of experiments, animals were only subjected to one (left or right) or both transient (50 minutes) CCAo, whereas others underwent definitively ligation of one or both CCA (referred to as model M2, M3, or M4 respectively; see Table 1). Sham animals were only subjected to carotid isolation and did not receive MCA electrocoagulation or transient CCA occlusion. Of 68 animals, 1 died in model M1, and 3 died in model M4 during the first 24 hours of recovery.

Arterial Blood Flow Monitoring Using Ultrasound Imaging

Rats subjected to model M2 ($n = 8$) were analyzed using ultrasound measurements via an echocardiograph (Vivid 7; GE Medical Systems Ultrasound, Horten, Norway) equipped with a 12-MHz linear transducer (12L) as reported previously.[10] Doppler spectral recordings in the right and left internal carotid arteries, basilar trunk, and posterior (P2 segment) cerebral arterie,[11] were evaluated 1) before surgery, 2) during ischemia, 3) after reperfusion, and 4) 24 hours later ($n = 8$). Data were then transferred to an ultrasound image workstation for subsequent analysis (PC EchoPAC; GE Medical Systems Ultrasound). The repeatability coefficient values for intraobserver repeatability were 1.5 cm s^{-1} for the peak systolic, 1.7 cm s^{-1} for the end-diastolic, and 1.7 cm s^{-1} for the mean blood flow velocity (mBFV) in ICA.

Regional CBF Monitoring

Cortical regional CBF (rCBF) was monitored in the MCA territory by laser Doppler flowmetry in the same animals that were monitored using ultrasound imaging ($n = 8$, group M2). A laser-Doppler probe (MP7b, Moor Instruments Ltd, Axminster, UK) was positioned on the parietal cortex, and rCBF was monitored using a Moor CBF device in each animal before (basal) and during arterial occlusion and 15 minutes after reperfusion ($n = 8$). The

relative changes in rCBF were expressed as percentage of the average basal level recorded over 15 minutes.

Assessment of Cell Damage

At 12, 48, and 72 hours after injury, the brains were removed, fixed and cryoprotected and cut into 20-μm-thick coronal sections. Sections through the dorsal hippocampus (bregma – 3.3 mm) were stained with cresyl-violet or processed either for terminal transferase-mediated dUTP nick-end labeling (TUNEL) staining according to the manufacturer's instructions (Roche, Meylan, France) or for Fluoro-Jade B (Histochem, Jefferson, AR) as reported previously.[12]

Immunohistochemistry

Immunohistochemistry was performed on cryostat coronal sections (at 4, 12, 24 (M1), 48 (M1 to M4) and 72 (M2) hours after injury) as previously described,[13] using anti-cleaved caspase-3 (casp3) (Asp175; Cell Signaling Technology, Ozyme, St-Quentin-en-Yvelines, France). Casp3-labeled cells were counted (in a blind manner) in both IL- and CL cortex in three to four coronal sections for each animal at 48 hours of recovery (n = 4–6) and in age-matched control (n = 2) rats, using a ×20 objective. Cleaved casp3 is found in the cytosol and becomes active after translocation in the nucleus.[14]

Simple and Double Immunofluorescence

Immunofluorescent staining was performed on free-floating sections (30 μm thick) as previously described,[15] using anti-cleaved casp3 (rabbit polyclonal ALX-210-807; Alexis Biochemicals, Coger, Paris, France), NeuN (VMA377; AbCys, Paris, France) to label neurons, glial fibrillary acidic protein (clone G-A-5; Sigma-Aldrich) to stain astrocytes, nestin (clone Rat 401; Chemicon, Euromedex, Souffelweyersheim, France), and vimentin (clone VIM 13.2; Sigma-Aldrich) to detect progenitor cells, and finally GABA (MAB351; Chemicon, Millipore, St-Quentin-en-Yvelines, France) to identify GABA interneurons. Selected sections were photographed using a Nikon Eclipse E800M microscope (Paris, France) and DFC 300 FX camera (Leica Microsystems, Rueil-Malmaison, France) interfaced with IM50 imaging software. 4′,6′-Diamidino-2-phenylindole labeling was used to visualize nuclear morphology. Double immunofluorescence (cell marker and cleaved casp3) staining was analyzed using a Leica TCS SP5 AOBS confocal laser microscope with a ×63 lens, and z-series stack (2-μm-optical slice thickness) images were obtained and imported into Adobe Photoshop (version 7.0) and ImageJ (1.38x; National Institutes of Health, Bethesda, MD) for image processing and analysis.

Western Blot Analysis

Sham (n = 2), model M1 (n = 6), and model M2 (n = 6) animals were sacrificed at 48 hours after injury and brains rapidly dissected out on a cold plate as reported previously.[16] Cortical tissues were harvested and stored to −70°C until use. To each tissue piece, 9 volumes of ice-cold homogenization buffer [15 mmol/L Tris-HCl (pH 7.6), 320 mmol/L sucrose, 3 mmol/L EDTA, 1 mmol/L DTT, and the protease inhibitor mixture (Roche)] were added. Cell lysates were then centrifuged at 800 × g for 10 minutes. at 4°C, given a supernatant (S1) and a pellet (P1, nuclear fraction). S1 was then centrifuged at 9200 × g for 20 minutes at 4°C, producing a crude cytosolic (S2) fraction in the supernatant and a mitochondrial fraction (M1). P1 and S2 fractions were solubilized, and an equal amount of protein (40 μg) was submitted to Western blotting. The primary antibodies used in this study were anti-casp2 (ALX-804-356; Alexis Biochemicals), casp8 (sc-5263), and cytochrome c (sc-13560) both from Santa Cruz Biotechnology (Tebu-Bio, Le Perray-en-Yvelines, France), cleaved casp9 (Asp^{353}) and casp3 (Asp^{175}), -Akt (number 9272) and -p-Akt (Ser^{473}), glycogen synthase kinase-3β (27C10) and -p-GSK-3β (Ser^{9}), Erk1/2 (number 9102), and -p-Erk1/2 (Thr^{202}/Tyr^{204}) all from Cell Signaling Technology. Antibodies against αII-spectrin (FG 6090; BIOMOL, Coger, Paris, France), poly(ADP-ribose) polymerase-1 (11835238001; Roche), and β-actin (clone AC-15; Sigma-Aldrich) were also used. The blots were semiquantified using gel densitometry and ImageJ analysis system. An absence of cyclophilin D (AP1035; Calbiochem, Merck Chemicals, Nottingham, UK) immunostaining in the cytosolic S2 fraction indicated that S2 was not contaminated with mitochondrial material.

Statistical Analysis

All results are expressed as mean ± SD. One-way analysis of variance and *post hoc* Bonferronni test were used to analyze differences between the groups (Western blotting analysis, laser Doppler measurements). A Kruskal-Wallis nonparametric test was used to analyze differences in peak systolic, end-diastolic, and time-average mBFVs measured in the right and left cerebral arteries. Pearson correlation analysis was used to reveal the correlation among the number of cleaved casp3-positive cells and the percentage of reperfusion. StatView 6.0 software was used in all statistical analyses.

Results

Neonatal Ischemia Triggers Cleavage of Casp3 in Both Hemispheres

No p17 cleaved casp3 immunoreactivity was found in the cortex of sham animals (data not shown). In contrast, casp3 labeling was detected in both IL and CL cortices in ischemic animals from the group M1, at 48 hours. In the CL cortex, casp3 was detected in the more caudal region (dorsal hippocampus) and exclusively in the cytosol of numerous cells present in layers IV to VI (Figure 1). However, DNA fragmentation in these regions was undetectable as evidenced by TUNEL assay (Figure 1, A–C

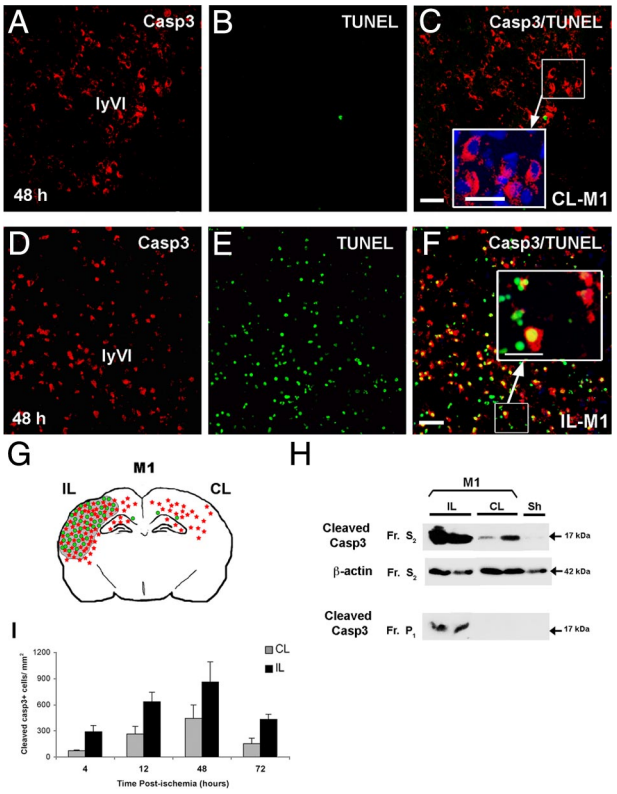

Figure 1. Neonatal ischemia triggers activation of caspase-3 (casp3) in both hemispheres. Cleaved casp3 immunolabeling (red) and TUNEL assay (DNA fragmentation, green) in sections of brain at the level of the dorsal hippocampus (bregma −3.3 mm) from contralateral (CL-M1, **A–C**) and ipsilateral (IL-M1, **D–F**) hemispheres at 48 hours postischemia (model M1). Note that active casp3 was cytosolic in the CL cortex (enlarged panel in **C**), whereas it was nuclear and cytosolic and associated with TUNEL staining in the IL cortex (enlarged panel in **F**). Scale bar represents 50 and 20 μm in enlarged panels. **G:** Spatial distribution of cleaved casp3- (red) and TUNEL-positive (green) cells and lesion area (gray) at 48 hours after ischemic injury in P7 rats in both IL and CL hemispheres. **H:** Representative Western blots probed with anti-active casp3 (17 kDa; Cell Signaling Technology) for protein samples isolated from the cytosolic (S2) and nuclear (P1) fractions of IL and CL cortex from ischemic rats sacrificed 48 hours after reperfusion and from sham (Sh) brain. The cytosolic marker β-actin was used as protein loading control. Note that p17 was present in the cytosolic fractions in both IL and CL tissues. In contrast, p17 was only present in the nuclear fraction for IL tissues; Fr, fraction. **I:** Quantification of casp3-positive cells at 4, 12, 48, and 72 hours postischemia in both IL and CL cortex.

and I). In contrast, cleaved casp3 was detected in a large number (~82–84%) of TUNEL-positive cells throughout cortical layers with a cytosolic and/or nuclear localization in the IL cortex (Figure 1, D–F and I). The number of cleaved casp3-positive cells increased from 4 to 48 hours (peak) in both IL and CL cortex with 861 ± 231 and 442 ± 154 positive cells at 48 hours, respectively (Figure 1G). The number of casp3-positive cells remained elevated in the IL cortex but not in the CL cortex at 3 days postinjury. Western blot analysis demonstrated that p17-cleaved casp3 was found in both cytosolic and nuclear fractions from IL cortical tissues and only in cytosolic fractions from CL cortices at 48 hours postinjury (Figure 1H); cleaved casp3 expression in the CL cortex only represented 15 to 25% (n = 8) of that detected in the IL cortex. It should be noted that sections from ischemic (model M1) animals treated with the pan-caspase inhibitor Q-VD-OPh (used in our previous study[16]) and analyzed 48 hours later demonstrated a very significant reduction in casp3-positive cells in the IL hemisphere and no labeling in the CL hemisphere (data not shown).

CCA Occlusion Triggers Casp3 Cleavage in Both Hemispheres

To determine the depth of hypoperfusion sufficient and required to produce cleaved casp3 without DNA fragmentation in the CL cortex, we tested blood flow perturbation induced by unilateral (uni) or bilateral (bi-) transient (t) or permanent (p) CCA occlusion (model M2 to M4; Table 1). As shown in supplemental Figure S1 (see *http://ajp.amjpathol.org*) with cresyl-violet staining at 48 hours postinjury, uni-tCCAo (supplemental Figure S1, A and B; n = 7), uni-pCCAo (data not shown, n = 5), and bi-tCCAo (supplemental Figure S1, C and D; n = 5) did not induce significant cell death. In contrast, a pale zone in cortical layer VI and white matter (external capsule; supplemental Fig. S1, E and F, see *http://ajp.amjpathol.org*; n = 7) was observed after Bi-pCCAo. Additionally, a pale zone in all cortical layers and white matter was observed after MCAo with uni-tCCAo (model

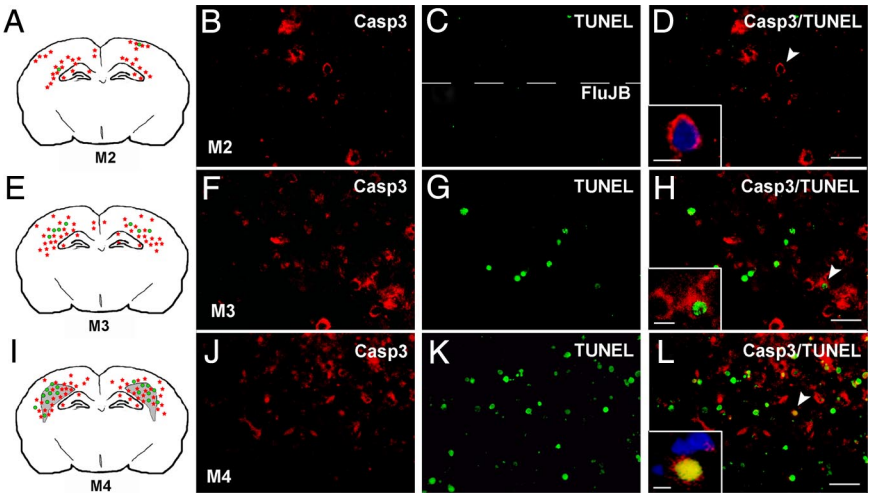

Figure 2. Casp3 cleavage and DNA fragmentation in several models of carotid occlusion at 48 hours after injury. Spatial distribution (**A**, **E**, and **I**) of cleaved casp3 (red), TUNEL-positive (green) cells, and lesion area (gray) after uni-CCAo (model M2), bi-tCCAo (model M3) and bi-pCCAo (model M4), respectively. Note that images in mirror were detected in all three ischemic conditions. Double fluorescent staining in the CL cortex for cleaved casp3 (**B**, **F**, and **J**) and TUNEL (**C**, **top**, **G**, and **K**) or Fluorojade B (FluJB) labeling (**C**, **bottom**). After uni-CCAo, only cytosolic cleaved casp3 (enlarged image in **D**) without TUNEL or FluJB staining was observed. In contrast, several cells displayed cytosolic cleaved casp3 co-localized with TUNEL staining (**F–H**, note chromatin clumps typical of apoptotic cells, enlarged panel in **H**) after model M3. A large number of cells exhibited both cytosolic and nuclear cleaved casp3 and DNA fragmentation after model M4 (**J–L**). Some sections were counterstained with 4′,6′-diamidino-2-phenylindole (overlay in **D** and **L**). Scale bar represents 50 and 20 μm (enlarged panels).

M1; supplemental Figure S1, G and H, see *http://ajp.amjpathol.org*; $n = 6$). All ischemic procedures induced cleavage of casp3 in both IL and CL cortices, and the labeling was observed in layers II–III and VI for the different models studied (Figure 2). No cell death (TUNEL and Fluoro Jade B staining) was found to be associated with the former (uni-tCCAo or uni-pCCAo, M2; Figure 2, A–D), whereas TUNEL-positive nuclei were detected to a lesser (bi-tCCAo, M3, Figure 2, E–H) or greater (bi-pCCAo, M4; Figure 2, I–L) extent. Furthermore, cleaved casp3 displayed a cytosolic (Figure 2H) and a nuclear (Figure 2L) location after bi-tCCAo (M3) and bi-pCCAo (M4), respectively. Interestingly, a pattern of cleaved casp3 was found as images in mirror (Figure 2, A, E, and I) in all of the studied models. Although brain injury and apoptosis in the immature brain has been previously shown to depend on gender,[16–18] subanalysis according to sex demonstrated that the presence of cleaved casp3 in both hemispheres did not depend on gender in the present study.

We then only focused our analysis on animals subjected to unilateral CCAo (model M2) to determine which type of cells displayed cleaved casp3 without death features at 48 hours postinjury for comparison with CL hemisphere of M1 animals. Indeed, the number of cleaved casp3-positive cells increased from 12 to 48 hours (peak) and moderately declined at 72 hours later. Using double immunofluorescence and confocal analysis, we observed that mainly neurons (labeled with NeuN; Figure 3, A and B) and immature cells (labeled with nestin, Figure 3, C and D; and vimentin, Figure 3, E and F) expressed cleaved casp3, but not astrocytes (data not shown), and in a similar manner both in IL and CL cortex as in the CL side of model M1 animals. Specific labeling was detected in cortical layers II–III and VI. Interestingly, most of cleaved casp3-positive cells in the neocortical layer III expressed GABA (Figure 3, G–I).

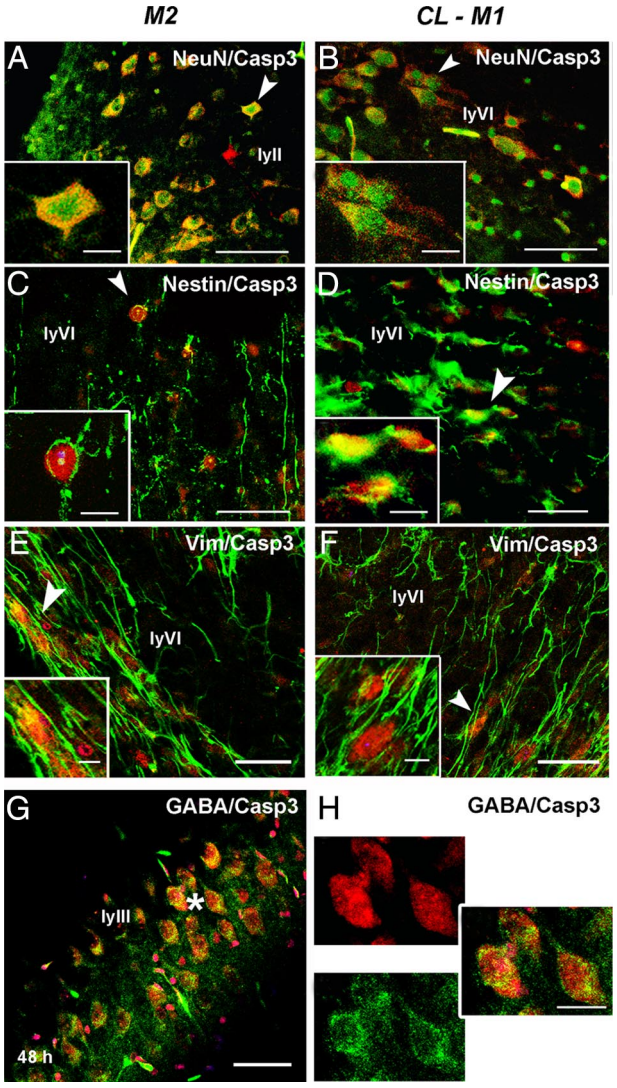

Figure 3. Unilateral transient CCA occlusion mainly triggers casp3 cleavage in neurons and undifferentiated cells in the P7 rat brain. Contralateral cortex from uni-CCAo (model M2) and MCAo + tCCAo (model M1) animals contain most cleaved casp3 colocalized with neurons (NeuN) (**A**, **B**), nestin- (**C**, **D**), and vimentin (**E**, **F**) positive cells **Arrows** indicate location magnified in **insets**. Co-localization of cleaved casp3 was observed in GABA-immunostained neurons in cortical layer III (ly III in **G**, and enlarged panels in **H**, indicated by the **asterisk** in **G**). Cleaved casp3 labeling is shown in red, whereas NeuN, nestin, vimentin and GABA markers are shown in green. Scale bar represents 50 and 20 μm (enlarged panels).

Molecular Pathways Involved in Cytosolic Casp3 Cleavage

Casp3 cleavage (and activation) has been reported in apoptosis[13,19] and preconditioning.[20] We therefore first evaluated by western blotting casp3 cleavage and subsequent cleavage of its substrates, such as α-II spectrin (fodrin) and poly (ADP-ribose) polymerase-1. At 48 hours after uni-tCCAo (Figure 4A), p17-cleaved casp3 and the 150-kDa α-II spectrin breakdown product, a marker of Ca^{2+}-mediated calpain activation, were detected (Figure 4C). This later appeared slightly (by ~25%) increased compared with sham tissues. Casp3-dependent spectrin cleavage, yielding p120 kDa breakdown product,[21] was only detected in the IL ischemic cortex but neither in the CL cortex after ischemia nor in both cortex tissues after uni-tCCAo. We then investigated upstream caspase (casp2, casp8, and casp9) cleavage, which could be involved in casp3 cleavage. Data reported in Figure 4B demonstrated that casp2 underwent cleavage until its small unit (17 kDa) after ischemia, in association with casp8 and casp9 cleavage, in the IL hemisphere. In the CL cortex after ischemia and in both cortex after uni-tCCAo, casp2 underwent an incomplete cleavage (absence of the 17-kDa fragment but presence of the 37- and 25-kDa fragments) without casp8 and casp9 cleavage. After ischemia, release of cytochrome *c* in the cytosol was more abundant that the one observed after uni-tCCAo. In contrast, cytochrome *c* release has not been detected in the CL cortex. It should be noted that no significant endogenous caspase inhibitor (survivin and c-IAP-2) proteins were up-expressed in cortical tissues from the CL ischemic brain (supplemental Figure S2, see *http://ajp.amjpathol.org*), whereas an increase was observed in the IL penumbra close to the infarct.

As the activation of both PI3K/Akt[22] and mitogen-activated protein kinase[23] signaling pathways were demon-

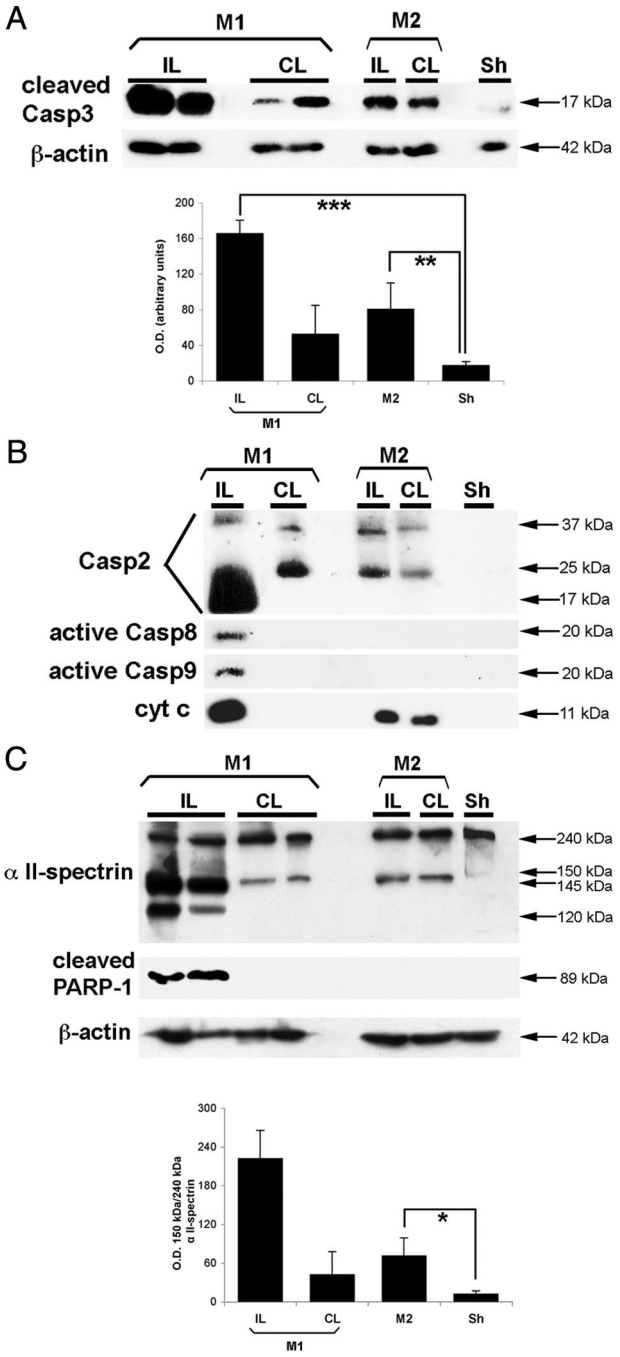

Figure 4. Unilateral transient CCA occlusion can induce casp3 cleavage but not its downstream subtracts. **A:** Representative Western blots showing cleaved casp3 fragment (17 kDa) both in the IL and CL 48 hours after uni-tCCAo + MCAo (model M1) and after uni-CCAo (model M2) as compared with sham-operated neocortical cytosolic extracts ($n = 8$ for each condition). Highly cleaved casp3 was present in the IL after model M1, but it also is increased in the CL cortex and after model M2 compared with sham (sh) cytosolic extracts ($P < 0.005$). The cytosolic marker β-actin was used as protein loading control. **B:** Upstream proapoptotic molecules are expressed after neonatal stroke (small units of casp2, casp8, and casp9). After uni-tCCAo, intermediate cleavage fragments of casp2 and cytosolic cytochrome *c* release were detected, as compared with sham animals. **C, upper panel:** Western blot showing calpain-cleaved fragments (150 to 145 kDa) and casp3-cleaved fragment (120 kDa) of α II-spectrin, and cleaved poly(ADP-ribose) polymerase-1 fragment (89 kDa). All these fragments were found in the IL extracts after model M1. In contrast, only the 150 kDa fragment was observed after model M2. **C, lower panel:** Quantification of the 150-kDa band (percentage between OD of the 150-kDa and total 240-kDa α II-spectrin). Data represent mean ± SEM ($n = 6$ each). $^{*}P < 0.05$; $^{**}P < 0.005$; and $^{***}P < 0.0001$.

strated to contribute to preconditioning-induced tolerance against hypoxic-ischemic brain injury, we evaluated those pathways after uni-tCCAo. An increase (~50%) only in p-ERK2 was detected after uni-tCCAo but not in pAkt and p-GSK-3β (Figure 5A). We then subjected animals to uni-CCAo and to a second ischemic injury (MCAo + uni-tCCAo) 24 hours after (model M5) and evaluated the lesion 48 hours after. This small increase in pERK2 was not sufficient to detect a difference in the mean score lesion between the two groups of animals (Figure 5B).

Blood Flow Monitoring and the Relation between Reperfusion and Cleaved Casp3-Positive Cells after uni-CCAo

To evaluate whether the role of CBF perturbations in bilateral neuronal cleaved casp3, blood flow status was monitored using two-dimensional color-coded pulsed Doppler ultrasound imaging in animals subjected to uni-CCA occlusion (model M2). In the basal state, heart rate of the rat pups was 352.4 ± 27.9 beats per minute. Unilateral transient occlusion (Uni-tCCAo) did not significantly modify heart rate value (332.5 ± 44.1, $n = 8$), which remained stable during the first day. For each artery studied, changes in peak systolic, and end diastolic BFVs followed changes in mBFVs (Figure 6). On basal state, all cerebral arteries mBFVs were similar between left and right sides in all eight animals. While left (IL) uni-tCCAo was maintained during 50 minutes, the left ICA (internal carotid artery) was reversed toward the external carotid artery in each of the eight animals. In contrast, the right (CL) ICA (internal carotid artery) and BT (basilar trunk) mBFVs significantly increased (by 40%, $P < 0.01$ and 39%, $P < 0.05$ versus basal values, respectively) in each of the eight animals to supply the arterial terminal branches of the left ICA, as well as the left external carotid artery through the anterior cerebral and posterior communicating arteries (Figure 6). Nevertheless, the left PCA (posterior carotid artery) declined by only 10% whereas in right PCA, mBFVs did not vary from their basal levels suggesting a hypoperfusion in the left hemisphere and the absence of hypoperfusion in the right hemisphere in all animals. Fifteen minutes after release of the left uni-tCCAo, left ICA was reinjected anterogradely in five of the eight rat pups but exhibited reduced mBFVs at 64% of basal level ($P < 0.05$), whereas all others mBFVs returned to basal values (Figure 6). These five animals displayed mBFVs values similar to basal control values 24 hours after ischemia. In the three remaining animals, left ICA remained occluded after release of the left uni-tCCAo. MBFVs in the right ICA then increased until 24 hours after ischemia (at 209% of basal values; Figure 6). To obtain data on rCBF in the MCA territory, laser Doppler flowmetry was performed on the same animals and others ($n = 3$) with ligated IL CCA to increase their number. We observed that during ischemia rCBF declined in the IL cortex (46.2 ± 9.7 versus basal value (noted as 100); $P < 0.05$) but not in the CL (90.6 ± 11.2 versus basal value, N.S; $P < 0.05$ versus IL).

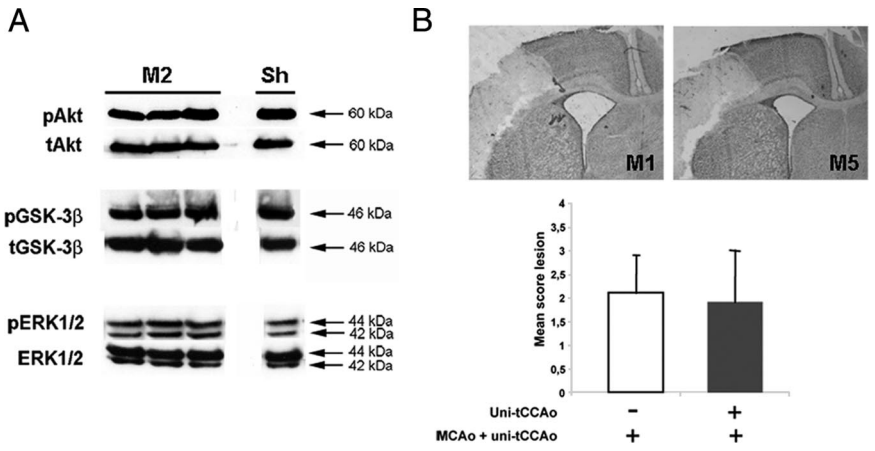

Figure 5. Unilateral transient CCA occlusion did not induce preconditioning. **A:** Representative Western blots showing p-Akt (60 kDa), p-GSK-3β (46 kDa), and p-ERK1/2 (42/44 kDa) in sham-operated (Sham) and uni-CCAo (model M2) neocortical cytosolic extracts at 48 hours postlesion compared with total (t) protein. No significant difference between M2 and sham-operated animals in p-Akt and p-GSK-3β was detected. An increase (~50%) in p-ERK2 was only detected. **B:** Effect of uni-tCCAo 24 hours before ischemia on the lesion score (lesion was graded from 0 to 3, where 0 indicated no observable lesion and 1, 2, and 3 indicated small, medium and large infarct, respectively, see Ref. [11]). Representative Cresyl-violet stained sections (**upper panels**) showing a similar pale zone in animals subjected to previous uni-tCCAo (model M5) as compared with ischemic animals (model M1). Lesion score also was similar in both groups (**lower panel**, $n = 6$, each).

No difference was observed between animals displaying reperfusion or not. Regional CBF values were 72.6 ± 24.5 and 97.8 ± 18.4, in the IL and CL, respectively, 30 minutes after reperfusion.

Interestingly, all animals displayed cleaved casp3 in both the IL and CL cortex (with no significant difference between both sides, $P = 0.338$) and no TUNEL but with a wide range in their number (between 300 and 998 per mm^2, with a mean of 547.7 ± 259.8 in the IL and 399.7 ± 110.2 in the CL hemisphere). The ratio of immediate left internal carotid reflow (from 0 to incomplete, 25 to 40%, or complete, 80 to 100%, as measured by ultrasonic imaging (supplemental Table S1, see *http://ajp.amjpathol.org*)) and the number of cleaved casp-3-positive cells appeared to be negatively correlated both in the IL ($R^2 = 0.627$, $P = 0.0207$) and surprisingly also in the CL ($R^2 = 0.727$, $P = 0.0147$) cortex, as we found mirror images. This correlation did not subsist at 24 hours after injury as we have two groups (one with complete reperfusion, one without).

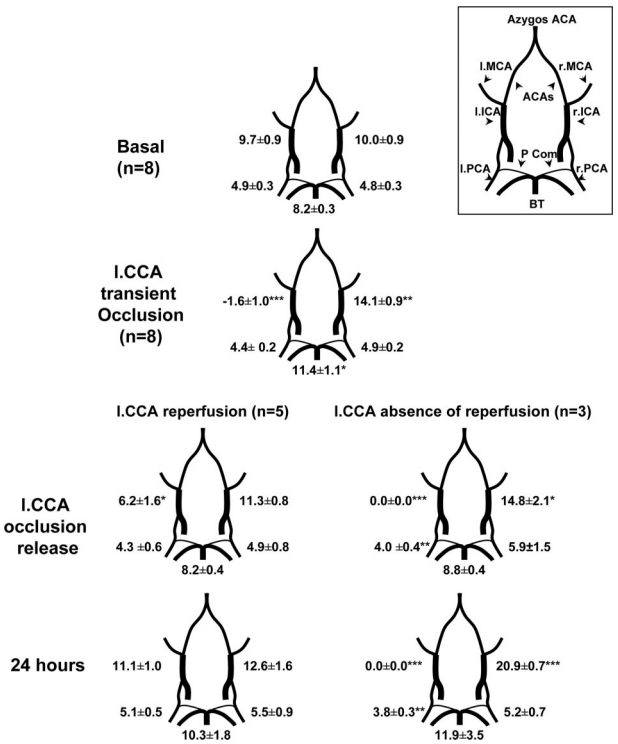

Figure 6. CBF monitoring using two-dimensional color-coded ultrasound imaging. Time-average mBFV 1) before, 2) during occlusion of the left CCA and 3) after CCAo release in eight animals. mBFVs (mean ± SEM, cm · s^{-1}) were measured in right (r) and left (l) posterior cerebral arteries (PCA, P2 segment) and internal carotid arteries (ICA), and in the basilar trunk (BT). During occlusion procedure, rat pups presented a reversed mBFV in the left ICA. After CCAo release, rat pups exhibited either reflow in the left ICA ($n = 5$) or not ($n = 3$). Data are mean ± SD *$P < 0.05$, **$P < 0.01$, ***$P < 0.001$ versus basal values. **Upper right:** Circle of Willis in the rat brain. ACA: anterior cerebral artery; Pcom, posterior communicants.

Discussion

The most commonly used model In P7 Wistar rats is HI, which was designed by Vannucci's group.[4] Arterial occlusion models, such as the one used in this study can be considered complementary since these models examine two different types of cerebral insults (HI injury and stroke). Unilateral stroke (model M1) in P7 rats induces neuronal cleaved casp3 in the CL cortex without DNA fragmentation at 48 hours. Surprisingly, a unilateral hypoperfusion alone (50 minutes left CCA occlusion), not sufficient to induce cell death, also produces delayed casp3 cleavage bilaterally and symmetrically giving images in mirror. To the best of our knowledge, this study represents the first demonstration that unilateral vascular occlusion induces transient collateral circulation and/or autoregulatory mechanisms producing delayed bilateral molecular pathways in the P7 rat brain.

Following ischemia in P7 rats, the CL cortex exhibited casp3 cleavage mainly in neurons in absence of any death marker (TUNEL and Fluoro-jade B staining) at 48 hours postinjury. Several studies have identified CL cell injury/death after HI in P7 rats.[24,25] However, these studies only pointed out early (2 and 4 hours) signs of apoptosis. More recently, Martin et al[26] found a significant number of P7 animals with CL cell death with casp3 activity 1 hour post-HI, but not later, that was not a direct extension of the IL injury. Early expression of molecules belonging to preconditioning (hypoxic-inducing factor-1α, p-Akt) in the CL hemisphere using the same HI model in P12 rats was also reported.[7] Although we cannot rule out that similar events occurred early after injury in the CL

side of ischemic animals, such events were not detected at 48 hours neither for p-Akt and p-GSK-3β nor for increased endogenous caspase inhibitors such as survivin[27] and IAPs.[28] Again, 48 hours after uni-tCCAo such survival pathways were not evidenced except for p-ERK2. These results led us to investigate apoptotic protagonists upstream to cleaved casp3 both in the CL hemisphere of ischemic animals and after uni-tCCAo. Data strongly suggested that apoptosis occurred through Ca^{2+}-dependent calpain.[29] As well, Ca^{2+}-dependent casp2 activation[30] is able to initiate mitochondrial membrane permeabilization, thus promoting cytochrome *c* release[31,32] independently of its enzymatic activity[33] or due to an upstream casp2-dependent redistribution of Bax from cytosol to mitochondria.[34] These results strongly suggest that IL hypoperfusion is insufficient to create an IL cortical lesion but sufficient to induce initiator signals (most likely intracellular Ca^{2+}) able to begin the process of apoptosis (casp2 cleavage and cytochrome *c* release) and to stop it before caspase substrate cleavage and expression of nuclear death markers in the CL cortex after ischemia and in both cortices after uni-tCCAo. However, it is important to note that released cytochrome *c* was not detected in the S2 cytosolic fraction from CL tissues taken from model M1. As the decline in casp3 labeling was faster in model M1 than that observed in model M2, we suspect that 48 hours postinjury was not the most appropriate time point to detect cytochrome *c* release in CL brain tissues from M1 rats. As ischemia (MCAo + uni-tCCAo, model M1) performed 24 hours after uni-CCAo produced an ischemic lesion similar to that classically observed, we suggest that cytosolic cleaved casp3 did not represent preconditioning but really aborted apoptosis.

Neonatal brains are different from adult brains. Interestingly, the age at insult (two first weeks of life) may be a determining factor in vascular responses, calcium regulation, and synaptogenesis: 1) Choy et al[35] reported age-dependent nature of vasculature remodeling in response to bilateral carotid occlusion (with larger collaterals in P3 neonatal than 2-month-old adult brains). 2) Vascular endothelial growth factor has an essential role for vessel growth in early postnatal life,[36] and there is a close correlation between cerebral angiogenesis and vascular endothelial growth factor expression in the postnatal developing brain (with a specific neuronal co-localization at P8 in layer IV and VI).[37] 3) Elevation in $[Ca^{2+}]_i$ has been proposed to be a critical event leading to activation of proteases, phospholipases, and endonucleases, which in turn may lead to necrotic or apoptotic cell death.[38] Given the robust increase in [Ca2+]i in P7 to P8 as compared with P13 and P20 rats and the slow decrease after HI, the temporal $[Ca^{2+}]$i change may provide a basis for developmental stage-specific injury[39] and mu-calpain activation.[40] 4) In the developmental brain, the ability of cytochrome *c* to induce cleavage and activation of caspase-3 is decreased during maturation in rat brain samples after 2 weeks of age.[41,42] 5) The first 20 postnatal days represent the period of rapid differentiation of axons and dendrites.[43] 6) Neonatal brains are more vulnerable to glutamate-mediated excitotoxicity than adult brains, possibly due to differences in the subunit composition of *N*-methyl-D-aspartate receptors.[44] Taken together, all of the above listed age-dependent cerebral properties may probably explain that many molecular pathways can be activated after a vascular occlusion at P7.

Thus, the question arose what is the *primum movens* in the appearance of CL neuronal cytosolic cleaved casp3 without nuclear DNA fragmentation after uni-tCCAo: 1) a modification of CBF velocities in arteries leading to a modified blood status in both cortexes during carotid occlusion or 2) a transmutation of neuronal signals from IL to CL cortex suggesting neuronal coupling?

During or after HI in P7 rats, blood flow in CL cerebral hemispheric structures was relatively unchanged from prehypoxic values[45,46] as quantified with autoradiographic iodo-[^{14}C]antipyrine technique, whereas flow to the brainstem and cerebellum nearly doubled and tripled, respectively.[47] In this study, we subjected animals to unilateral CCA occlusion alone and monitored CBF using two-dimensional color-coded pulsed and laser Doppler. All rat pups with an IL hypoperfusion exhibited an early rise in BT and right ICA mBFVs during ischemia. This rise helps to compensate the abolition of the left ICA blood flow rate during left CCA occlusion and mirrors 1) the efficiency of collateral blood flow supply through the communicating arteries of the circle of Willis as described in human,[48] and 2) the fast opening of cortical arterial anastomoses between anterior, middle and posterior territories.[6,9,48,49] The number and size of these anastomotic vessels are greatest between anterior and middle cerebral arteries, with smaller and fewer connections between middle and posterior cerebral arteries and even less prominent terminal anastomoses between posterior and anterior cerebral arteries.[9] Establishment of blood flow through the communicating arteries and the cortical collateral anastomoses proceeds from the oxidative metabolism in the ischemic area.[50] Maintenance and increment of this collateral blood flow supply is mediated by the arterial nitric oxide from endothelial nitric oxide synthase activation implied in vasodilation.[51] After reperfusion in the IL CCA, mBFVs return to basal values in animals exhibiting reperfusion in the IL CCA, whereas those without reperfusion still displayed a supplementary rise in CL ICA mBFVs, but a basal rCBF. All animals, however, displayed cleaved-casp3 in both IL and CL cortex at 48 hours after t-CCAo with a mean number similar to that previously obtained in the CL cortex after ischemia (547.7 $\pm$ 259.8 versus 442 $\pm$ 154; NS), although DNA fragmentation has not been found. Symmetric data were obtained with right CCA transient occlusion and normal CBF measurements in the left cortex leading to symmetric cleaved casp3 (data not shown). Therefore, no CL hypoperfusion in the MCA territory could explain upstream apoptotic activation. As we found a negative correlation between the level of reflow in the CCA and casp3-positive neurons, the absence of reperfusion in the IL CCA alone is responsible to a greater number of labeled cells in both IL and CL cortices in the model M2 and likely in a similar way in the model M1.

Martin et al[26] suggested that very early apoptosis in the CL cortex might involve CL exposure to soluble factor(s) released into the cerebral spinal fluid as a result of

IL injury. To further investigate the relationship between the early IL hemodynamic stress and the delayed (48 hours) casp3 cleavage in the unaffected cortex giving images in mirror we focused on the nature of cleaved casp3-positive neurons. Casp3-labeled neurons were mainly located in layers II–III and VI and most of them were GABAergic interneurons in layer III (see Figure 3) and we suggested that those present in layer VI could be mainly glutamatergic.[52] In the brain, neurovascular interactions occur in the hemodynamic changes (vasoconstriction and/or vasodilation) and represent what is called neurovascular coupling. Alterations in the release of both inhibitory (GABA) and excitatory (glutamate) neurotransmitters were observed, and have been recently reported in the hemisphere CL to stroke.[53] The ability of specific subsets of cortical GABA interneurons to transmute neuronal signals into vascular responses was also demonstrated and further suggested that they could act as local integrators of neurovascular coupling for subcortical vasoactive pathways.[54] In addition, a subgroup of GABAergic neurons, distributed throughout the neocortex, has been reported to project over long distances in several species with axon branches traveled rostro-caudally and medio-laterally,[55–57] making them a part of a corticocortical network. Again, the overwhelming majority of long-distance connections in the cerebral cortex also originate from glutamatergic pyramidal neurons, which predominantly project cortico-cortically toward IL or CL targets.[58] Taken together, our data suggest that unilateral hypoperfusion induced increased intracellular Ca^{2+} (activating Ca^{2+}-dependent proteases) and/or factors (glutamate, GABA) most likely secreted by some of GABAergic and glutamatergic neurons, which might transmute signals either by their own long projections or by transcallosal fibers in the unaffected brain side. Those signals only represent a mild stress leading to moderate casp3 cleavage and incomplete apoptosis in the immature brain.

Hypoperfusion (diaschisis, steal syndrome) and/or hyperperfusion (luxury syndrome) were associated with cerebrovascular diseases. In the human adult, transcallosal diaschisis with "mirror effect" after unilateral stroke[59,60] and sustained mirror movements that involve the unaffected motor cortex[61] was reported. In human infants, it is known that loss of autoregulation and/or hyperperfusion syndrome after asphyxia can foreshadow an adverse outcome.[62] However, similar syndromes are difficult to establish in rodents and such bilateral molecular mechanisms described here only represent the consequence of hemodynamic perturbations in the immature rat brain.

We conclude that a transient unilateral (IL) hemodynamic stress could induce a transient increase in CBF velocities in the opposite hemisphere and delayed cleavage of neuronal casp3 in both IL and CL cortices producing images in mirror. This molecular response probably occurs by an IL energetic deficit and an increased in intracellular Ca^{2+} in local GABA interneurons (in layer II–III) and glutamatergic neurons (in layer VI) that can, at least in part, transmute those signals to the CL side either by transcallosal fibers and/or directly by their long-distance axons. The exact mechanisms causing this mirror effect await further clarification but to produce corpus-callosectomy in immature animals at the moment appears difficult to achieve. Additionally, an important finding from this study is that the opposite healthy hemisphere is not the same as it was before the injury and should not be used in such models as an internal control.

Acknowledgments

We are indebted to IFR83 Cell Imaging Facility for their valuable assistance. Todd James Treangen is thanked for revising the manuscript.

References

1. Ferriero DM: Neonatal brain injury. N Engl J Med 2004, 351:1985–1995
2. Golomb MR, Garg BP, Saha C, Azzouz F, Williams LS: Cerebral palsy after perinatal arterial ischemic stroke. J Child Neurol 2008, 23:279–286
3. Lynch JK, Hirtz DG, DeVeber G, Nelson KB: Report of the National Institute of Neurological Disorders and Stroke workshop on perinatal and childhood stroke. Pediatrics 2002, 109:116–123
4. Rice JE 3rd, Vannucci RC, Brierley JB: The influence of immaturity on hypoxic-ischemic brain damage in the rat. Ann Neurol 1981, 9:131–141
5. Derugin N, Ferriero DM, Vexler ZS: Neonatal reversible focal cerebral ischemia: a new model. Neurosci Res 1998, 32:349–353
6. Renolleau S, Aggoun-Zouaoui D, Ben-Ari Y, Charriaut-Marlangue C: A model of transient unilateral focal ischemia with reperfusion in the P7 neonatal rat: morphological changes indicative of apoptosis, Stroke 1998, 29:1454–1460; discussion 1461
7. van den Tweel ER, Kavelaars A, Lombardi MS, Nijboer CH, Groenendaal F, van Bel F, Heijnen CJ: Bilateral molecular changes in a neonatal rat model of unilateral hypoxic-ischemic brain damage. Pediatr Res 2006, 59:434–439
8. Spiegler M, Villapol S, Biran V, Goyenvalle C, Mariani J, Renolleau S, Charriaut-Marlangue C: Bilateral changes after neonatal ischemia in the P7 rat brain. J Neuropathol Exp Neurol 2007, 66:481–490
9. Liebeskind DS: Collateral circulation. Stroke 2003, 34:2279–2284
10. Bonnin P, Debbabi H, Mariani J, Charriaut-Marlangue C, Renolleau S: Ultrasonic assessment of cerebral blood flow changes during ischemia-reperfusion in 7-day-old rats. Ultrasound Med Biol 2008, 34:913–922
11. Hilger T, Niessen F, Diedenhofen M, Hossmann KA, Hoehn M: Magnetic resonance angiography of thromboembolic stroke in rats: indicator of recanalization probability and tissue survival after recombinant tissue plasminogen activator treatment. J Cereb Blood Flow Metab 2002, 22:652–662
12. Joly LM, Mucignat V, Mariani J, Plotkine M, Charriaut-Marlangue C: Caspase inhibition after neonatal ischemia in the rat brain. J Cereb Blood Flow Metab 2004, 24:124–131
13. Benjelloun N, Joly LM, Palmier B, Plotkine M, Charriaut-Marlangue C: Apoptotic mitochondrial pathway in neurones and astrocytes after neonatal hypoxia-ischaemia in the rat brain. Neuropathol Appl Neurobiol 2003, 29:350–360
14. Marks N, Berg MJ: Recent advances on neuronal caspases in development and neurodegeneration. Neurochem Int 1999, 35:195–220
15. Villapol S, Acarin L, Faiz M, Castellano B, Gonzalez B: Survivin and heat shock protein 25/27 colocalize with cleaved caspase-3 in surviving reactive astrocytes following excitotoxicity to the immature brain. Neuroscience 2008, 153:108–119
16. Renolleau S, Fau S, Goyenvalle C, Joly LM, Chauvier D, Jacotot E, Mariani J, Charriaut-Marlangue C: Specific caspase inhibitor Q-VD-OPh prevents neonatal stroke in P7 rat: a role for gender. J Neurochem 2007, 100:1062–1071
17. Hagberg H, Wilson MA, Matsushita H, Zhu C, Lange M, Gustavsson M, Poitras MF, Dawson TM, Dawson VL, Northington F, Johnston MV: PARP-1 gene disruption in mice preferentially protects males from perinatal brain injury. J Neurochem 2004, 90:1068–1075
18. Johnston MV, Hagberg H: Sex and the pathogenesis of cerebral palsy. Dev Med Child Neurol 2007, 49:74–78
19. Manabat C, Han BH, Wendland M, Derugin N, Fox CK, Choi J,

Holtzman DM, Ferriero DM, Vexler ZS: Reperfusion differentially induces caspase-3 activation in ischemic core and penumbra after stroke in immature brain. Stroke 2003, 34:207–213
20. Tanaka H, Yokota H, Jover T, Cappuccio I, Calderone A, Simionescu M, Bennett MV, Zukin RS: Ischemic preconditioning: neuronal survival in the face of caspase-3 activation. J Neurosci 2004, 24:2750–2759
21. Nath R, Huggins M, Glantz SB, Morrow JS, McGinnis K, Nadimpalli R, Wanga KK: Development and characterization of antibodies specific to caspase-3-produced αII-spectrin 120 kDa breakdown product: marker for neuronal apoptosis. Neurochem Int 2000, 37:351–361
22. Yin W, Signore AP, Iwai M, Cao G, Gao Y, Johnnides MJ, Hickey RW, Chen J: Preconditioning suppresses inflammation in neonatal hypoxic ischemia via Akt activation. Stroke 2007, 38:1017–1024
23. Wang X, Zhu C, Qiu L, Hagberg H, Sandberg M, Blomgren K: Activation of ERK1/2 after neonatal rat cerebral hypoxia-ischaemia. J Neurochem 2003, 86:351–362
24. Hill IE, MacManus JP, Rasquinha I, Tuor UI: DNA fragmentation indicative of apoptosis following unilateral cerebral hypoxia-ischemia in the neonatal rat. Brain Res 1995, 676:398–403
25. Joashi UC, Greenwood K, Taylor DL, Kozma M, Mazarakis ND, Edwards AD, Mehmet H: Poly(ADP ribose) polymerase cleavage precedes neuronal death in the hippocampus and cerebellum following injury to the developing rat forebrain. Eur J Neurosci 1999, 11:91–100
26. Martin SS, Perez-Polo JR, Noppens KM, Grafe MR: Biphasic changes in the levels of poly(ADP-ribose) polymerase-1 and caspase 3 in the immature brain following hypoxia-ischemia. Int J Dev Neurosci 2005, 23:673–686
27. Johnson EA, Svetlov SI, Wang KK, Hayes RL, Pineda JA: Cell-specific DNA fragmentation may be attenuated by a survivin-dependent mechanism after traumatic brain injury in rats. Exp Brain Res 2005, 167:17–26
28. Peng H, Huang Y, Duan Z, Erdmann N, Xu D, Herek S, Zheng J: Cellular IAP1 regulates TRAIL-induced apoptosis in human fetal cortical neural progenitor cells. J Neurosci Res 2005, 82:295–305
29. Blomgren K, McRae A, Bona E, Saido TC, Karlsson JO, Hagberg H: Degradation of fodrin and MAP 2 after neonatal cerebral hypoxic-ischemia. Brain Res 1995, 684:136–142
30. Amoroso S, D'Alessio A, Sirabella R, Di Renzo G, Annunziato L: Ca^{2+}-independent caspase-3 but not Ca^{2+}-dependent caspase-2 activation induced by oxidative stress leads to SH-SY5Y human neuroblastoma cell apoptosis. J Neurosci Res 2002, 68:454–462
31. Lassus P, Opitz-Araya X, Lazebnik Y: Requirement for caspase-2 in stress-induced apoptosis before mitochondrial permeabilization. Science 2002, 297:1352–1354
32. Robertson JD, Enoksson M, Suomela M, Zhivotovsky B, Orrenius S: Caspase-2 acts upstream of mitochondria to promote cytochrome *c* release during etoposide-induced apoptosis. J Biol Chem 2002, 277:29803–29809
33. Robertson JD, Gogvadze V, Kropotov A, Vakifahmetoglu H, Zhivotovsky B, Orrenius S: Processed caspase-2 can induce mitochondria-mediated apoptosis independently of its enzymatic activity. EMBO Rep 2004, 5:643–648
34. Chauvier D, Lecoeur H, Langonne A, Borgne-Sanchez A, Mariani J, Martinou JC, Rebouillat D, Jacotot E: Upstream control of apoptosis by caspase-2 in serum-deprived primary neurons. Apoptosis 2005, 10:1243–1259
35. Choy M, Ganesan V, Thomas DL, Thornton JS, Proctor E, King MD, van der Weerd L, Gadian DG, Lythgoe MF: The chronic vascular and haemodynamic response after permanent bilateral common carotid occlusion in newborn and adult rats. J Cereb Blood Flow Metab 2006, 26:1066–1075
36. Gerber HP, Hillan KJ, Ryan AM, Kowalski J, Keller GA, Rangell L, Wright BD, Radtke F, Aguet M, Ferrara N: VEGF is required for growth and survival in neonatal mice. Development 1999, 126:1149–1159
37. Ogunshola OO, Stewart WB, Mihalcik V, Solli T, Madri JA, Ment LR: Neuronal VEGF expression correlates with angiogenesis in postnatal developing rat brain. Brain Res Dev Brain Res 2000, 119:139–153
38. Kristian T, Ouyang Y, Siesjo BK: Calcium-induced neuronal cell death in vivo and in vitro: are the pathophysiologic mechanisms different? Adv Neurol 1996, 71:107–113; discussion 113–108
39. Takita M, Puka-Sundvall M, Miyakawa A, Hagberg H: In vivo calcium imaging of cerebral cortex in hypoxia-ischemia followed by developmental stage-specific injury in rats. Neurosci Res 2004, 48:169–173
40. Yamashima T, Saido TC, Takita M, Miyazawa A, Yamano J, Miyakawa A, Nishijyo H, Yamashita J, Kawashima S, Ono T, Yoshioka T: Transient brain ischaemia provokes Ca^{2+}: PIP2 and calpain responses prior to delayed neuronal death in monkeys. Eur J Neurosci 1996, 8:1932–1944
41. Wang X, Karlsson JO, Zhu C, Bahr BA, Hagberg H, Blomgren K: Caspase-3 activation after neonatal rat cerebral hypoxia-ischemia. Biol Neonate 2001, 79:172–179
42. Yakovlev AG, Ota K, Wang G, Movsesyan V, Bao WL, Yoshihara K, Faden AI: Differential expression of apoptotic protease-activating factor-1 and caspase-3 genes and susceptibility to apoptosis during brain development and after traumatic brain injury. J Neurosci 2001, 21:7439–7446
43. Dobbing J: Undernutrition and the developing brain. The relevance of animal models to the human problem. Bibl Nutr Dieta 1972, 35–46
44. McDonald JW, Johnston MV: Physiological and pathophysiological roles of excitatory amino acids during central nervons system development. Brain Res Brain Res Rev 1990, 15:41–70
45. Ringel M, Bryan RM, Vannucci RC: Regional cerebral blood flow during hypoxia-ischemia in the immature rat: comparison of iodoantipyrine and iodoamphetamine as radioactive tracers. Brain Res Dev Brain Res 1991, 59:231–235
46. Mujsce DJ, Christensen MA, Vannucci RC: Cerebral blood flow and edema in perinatal hypoxic-ischemic brain damage. Pediatr Res 1990, 27:450–453
47. Vannucci RC, Lyons DT, Vasta F: Regional cerebral blood flow during hypoxia-ischemia in immature rats. Stroke 1988, 19:245–250
48. van Laar PJ, Hendrikse J, Klijn CJ, Kappelle LJ, van Osch MJ, van der Grond J: Symptomatic carotid artery occlusion: flow territories of major brain-feeding arteries. Radiology 2007, 242:526–534
49. Menzies SA, Hoff JT, Betz AL: Middle cerebral artery occlusion in rats: a neurological and pathological evaluation of a reproducible model. Neurosurgery 1992, 31:100–106; discussion 106–107
50. Vannucci RC, Vannucci SJ: Glucose metabolism in the developing brain. Semin Perinatol 2000, 24:107–115
51. Zhang J, Snyder SH: Nitric oxide in the nervous system. Annu Rev Pharmacol Toxicol 1995, 35:213–233
52. Andjelic S, Gallopin T, Cauli B, Hill EL, Roux L, Badr S, Hu E, Tamas G, Lambolez B: Glutamatergic nonpyramidal neurons from neocortical layer VI and their comparison with pyramidal and spiny stellate neurons. J Neurophysiol 2009, 101:641–654
53. Skov-Madsen G, Christensen DM, Ruterbories J, Jensen W: Investigation of occurrence of lateralization in response to an ischemic stroke in rats. Conf Proc IEEE Eng Med Biol Soc 2008, pp 1–5
54. Cauli B, Tong XK, Rancillac A, Serluca N, Lambolez B, Rossier J, Hamel E: Cortical GABA interneurons in neurovascular coupling: relays for subcortical vasoactive pathways. J Neurosci 2004, 24:8940–8949
55. Higo S, Udaka N, Tamamaki N: Long-range GABAergic projection neurons in the cat neocortex. J Comp Neurol 2007, 503:421–431
56. Tomioka R, Okamoto K, Furuta T, Fujiyama F, Iwasato T, Yanagawa Y, Obata K, Kaneko T, Tamamaki N: Demonstration of long-range GABAergic connections distributed throughout the mouse neocortex. Eur J Neurosci 2005, 21:1587–1600
57. Tomioka R, Rockland KS: Long-distance corticocortical GABAergic neurons in the adult monkey white and gray matter. J Comp Neurol 2007, 505:526–538
58. Zhang ZW, Deschenes M: Intracortical axonal projections of lamina VI cells of the primary somatosensory cortex in the rat: a single-cell labeling study. J Neurosci 1997, 17:6365–6379
59. Dobkin JA, Levine RL, Lagreze HL, Dulli DA, Nickles RJ, Rowe BR: Evidence for transhemispheric diaschisis in unilateral stroke. Arch Neurol 1989, 46:1333–1336
60. Iglesias S, Marchal G, Rioux P, Beaudouin V, Hauttement AJ, de la Sayette V, Le Doze F, Derlon JM, Viader F, Baron JC: Do changes in oxygen metabolism in the unaffected cerebral hemisphere underlie early neurological recovery after stroke? A positron emission tomography study. Stroke 1996, 27:1192–1199
61. Kim YH, Jang SH, Chang Y, Byun WM, Son S, Ahn SH: Bilateral primary sensori-motor cortex activation of post-stroke mirror movements: an fMRI study. Neuroreport 2003, 14:1329–1332
62. Wintermark P, Moessinger AC, Gudinchet F, Meuli R: Perfusion-weighted magnetic resonance imaging patterns of hypoxic-ischemic encephalopathy in term neonates. J Magn Reson Imaging 2008, 28: 1019–1025